A sensitive magnetic arsenite-specific biosensor hosted in magnetotactic bacteria

Anissa DIEUDONNE[1], *Sandra PREVERAL*[1]*, *David PIGNOL*[1]*

[1]Aix Marseille Univ, CEA, CNRS, BIAM, UMR 7265, Saint Paul-Lez-Durance France

*Corresponding authors, Email address: sandra.preveral@cea.fr or david.pignol@cea.fr

Abstract

According to the World Health Organization, arsenic is the water contaminant that affects the largest number of people worldwide. To limit its impact on the population, cheap, quick and easy systems of detection are required. One promising solution could be the use of whole-cell biosensors, which have been extensively studied and could meet all these criteria even though they often lack sensitivity. Here we investigated the benefit of using of Magnetotactic Bacteria as cellular chassis to design and build sensitive magnetic bacterial biosensors. Promoters potentially inducible by arsenic were first identified *in silico* within the genomes of two magnetotactic bacteria strains: *Magnetospirillum magneticum* AMB-1 and *Magnetospirillum gryphiswaldense* MSR-1. The ArsR-dependent regulation was confirmed by reverse transcription PCR experiments. Biosensors built by transcriptional fusion between the arsenic-inducible promoters and the bacterial luciferase *luxCDABE* operon gave an element-specific response in 30 minutes with an arsenite detection limit of 0.5 µM. After magnetic concentration, we improved the

sensitivity of the biosensor by a factor of 50 to reach 10 nM, more than one order of magnitude below the recommended guidelines for arsenic in drinking water (0.13 µM). Finally, we demonstrated the successful preservation of the magnetic bacteria biosensors by freeze-drying

Importance

Whole-cell biosensors based on reporter genes can be designed for heavy metal detection but often require the optimization of their sensitivity and specific adaptations for practical use in the field. Magnetotactic bacteria as cellular host for biosensor are interesting models as their intrinsic magnetism allows an easy concentration and entrapment to increase the arsenic-response signal. This paves the way for the development of sensitive and immobilized whole-cell biosensors tailored for use in the field.

Keywords

Whole-cell biosensor; magnetotactic bacteria; arsenic; freeze-drying

Abbreviations

WHO, World Health Organization; MTB, magnetotactic bacteria; DAP, diaminopimelic acid; AMB-1, *Magnetospirillum magneticum*; MSR-1, *Magnetospirillum gryphiswaldense*

INTRODUCTION

Numerous environmental pollutants, including endocrine disruptors (1), plastics (2) but also heavy metals (3), pose a significant human health risk worldwide (4). Among them is arsenic, one of the most important chemicals to monitor in drinking water for health and safety issues according to the World Health Organization (WHO). Despite its high toxicity and occurrence in many parts of the world, arsenic concentrations in risky areas are often not monitored because of the high cost and lack of portable analytical techniques (5).

The use of microbial whole-cell biosensors could be a complementary, easy-to-use and inexpensive approach for the specific and semi-quantitative detection of arsenic. Many bacterial whole-cell biosensors described in the literature are derived from natural resistance mechanisms, containing a genetic regulation system. It consists in the coupling between a transcriptional regulator and a promoter rerouted for biosensor technology to control the expression of a reporter gene. Four induced bacterial metabolic pathways have been described in the presence of arsenic (6): the *arsRDABC* operon encoding a reductase and an efflux pump responsible for the export of inorganic arsenite out of the cell, methylation systems with an arsenite S-adenosylmethionine methyltransferase (ArsM) that can methylate arsenite, and two respiratory pathways based either on the oxidation of arsenite (As(III)) to arsenate (As(V)) (*aio*/*arx* genes) or the reduction of As(V) to As(III) (*arr* genes). The regulation of the *ars* operon is the most described (6). Its expression is genetically controlled by the ArsR regulator protein: in the absence of arsenic, this repressor binds DNA as a dimer and prevents transcription while in the presence of arsenic, the affinity of the ArsR-metalloid complex for the genomic operator decreases, allowing transcription and therefore signal translocation.

Numerous arsenic biosensors based on the ArsR regulatory system were described using reporter genes encoding either light emission protein (e.g., luciferase) or fluorescent protein (e.g., green fluorescent protein) (7). Most of them are hosted in *Escherichia coli* cells, allowing arsenic detection in less than one hour (8), with high specificity and a detection limit as low as 13 nM (0.1 µg/L) (9). Much progress has been made to improve the performance of biosensors compared to their conventional chemical counterparts, but their commercialization and field use have not yet fully matured. Various semi-autonomous in-line water analyzers using luminescent whole-cell biosensors have been described (10, 11), but cell preservation, immobilization and concentration with highly sensitive measurement maintained in the field, remains a major challenge.

In this study, we investigated the capacity of magnetotactic bacteria (MTB) to be tailored as luminescent biosensors. MTB comprise a group of taxonomically, physiologically, and morphologically diverse prokaryotes, with the unique ability to synthesize ferromagnetic nanoparticles that allow them to orient and move along the lines of the Earth's magnetic field (12–14). This magnetotactic property is due to the biomineralization of iron-rich magnetic nanocrystals embedded in lipidic vesicles forming an organelle called the magnetosome (13). The alignment of 15 to 20 magnetosomes in the cytoplasm acts like a compass needle to orient bacteria in geomagnetic fields, simplifying their search for preferred microaerobic environments (15). Many biotechnological applications exploiting this unique magnetic property are being developed, both in the medical and environmental fields (16). Here, we extend the scope of applications to environmental monitoring and report that *Magnetospirillum magneticum* AMB-1 (17) and *Magnetospirillum gryphiswaldense* MSR-1 (18) can be genetically modified to allow arsenic-dependent expression of transcriptional lux-based reporter gene. This study demonstrates

80 the strong potential of MTB for the development of sensitive and magnetically-guided whole-cell
81 biosensors.

Applied and Environmental Microbiology

MATERIALS AND METHODS

Strains and culture conditions. Strains and plasmids are presented in Table 1. *Magnetospirillum magneticum* AMB-1 strains were cultured at 28 °C in 1.5 mM MagMin medium (19) with 10 mg/L of kanamycin when required. *Magnetospirillum gryphiswaldense* MSR-1 strains were cultured at 28 °C in Flask Standard Medium (20) with 50 µM of iron citrate and 10 mg/L of kanamycin when required. The media for AMB-1 and MSR-1 were equilibrated at 2% of oxygen (flushed in the medium for AMB-1 and headspace for MSR-1) before inoculation. *Escherichia coli* DH5α was cultured in Luria Broth (LB) at 37 °C supplemented with 50 mg/L of kanamycin. *E. coli* WM3064 was cultured in LB with 50 mg/L of kanamycin and 0.3 mM of diaminopimelic acid (DAP). The magnetism of the different strains was spectrophotometrically estimated by calculating the coefficient of magnetism (C_{mag}) as previously described (21, 22).

Bacterial metal and metalloid resistance. Bacterial growth was monitored after the addition of different metal(loid)s (As(III), Cd(II), Co(II), Cu(II), Hg(II), Mo(VI), Ni(II), Sb(III) and Zn(II)) (Table S1) in a broad range of concentrations. One hundred µL of bacterial culture (OD_{600} = 0.1 for AMB-1 and OD_{600} = 0.5 for MSR-1) and 100 µL of growth medium supplemented with different metal(loid) concentrations were mixed in 96-well plates and incubated at 30 °C. The absorbance at 600 nm was measured with a microplate reader Infinite® 200 PRO (TECAN) every 30 minutes for 20 hours. Growth rates were calculated by linear regression and the half maximal inhibitory concentrations (IC_{50}) were estimated with a linear regression between the two metal(loid) concentrations flanking the half maximum growth rate. The experiment was repeated in triplicates on three different cultures. The given IC_{50} are

104 calculated as the mean of the three independent experiments, the error corresponds to the
105 standard deviation of the three values.

106 **Genomic analysis.** AMB-1 (NC_007626.1) and MSR-1 (MGMSR.2) genomes were
107 analyzed with the MaGe platform (Microbial Genome Annotation & Analysis) (27).
108 Identification of genes putatively involved in arsenic resistance was performed either by a search
109 for annotated genes whose name contained "ars" and by a blast analysis using the *E. coli* ArsR
110 protein sequence (access P15905 in Uniprot) as a template. Genes located around the identified
111 targets were subsequently analyzed and blasted with ArsA, ArsB, ArsC and ArsD protein
112 sequences from the *E. coli* arsenic resistance operon and ArsC from *S. aureus* arsenic resistance
113 operon. Jalview (28) was used for the final alignments of ArsR and ArsC. Sequence homology
114 percentages were calculated using the Ident and the Sim software (29). The genomes were
115 displayed with Gview (30).

116 **Transcriptional analysis.** AMB-1 and MSR-1 cells were grown in 1 L and 200 mL flasks,
117 respectively. When the cultures reached the mid-logarithmic growth phase, arsenite was added at
118 0, 50 or 200 µM. For each concentration, aliquots containing 10^{10} to 10^{11} cells were sampled at
119 five different times ranging from 0 to 30 hours. Total RNA was isolated using the ReliaPrep™
120 RNA Cell Miniprep System (Promega). Residual genomic DNA was removed with DNAseI
121 (Ambion). Extracted RNA was quantified with Nanodrop™. For each sample, 200 ng of RNA
122 were reverse-transcripted using SuperScript® VILO™ cDNA Synthesis kit and targeted genes
123 were amplified by PCR with Gotaq enzyme (Promega) and designed primers (Table 2). For each
124 pair of primers, a negative control was conducted with water and a positive control with genomic
125 DNA.

126 **Plasmid constructions.** pBBr_Lux, pBBr_Venus and $pArs_{Ecoli}$_Venus plasmids were
127 constructed by restriction enzyme cloning. The *luxCDABE* operon was inserted using a *SpeI*

digestion and the gene encoding the Venus protein was inserted as an *EcoRI/SacI* digestion. pArs$_{Ecoli}$ was amplified by PCR and inserted by *BamHI/HindIII* digestion upstream the Venus gene. The constructions for the other biosensors were made using a type IIS enzyme, *BsaI* (31). The backbone pBBR1-MCS2 was modified to harbor only two *BsaI* recognition sequences enclosing the lacZ gene. The arsenic promoters and *arsR* genes were amplified from the bacterial genomes (Table 2). The list of the resulting constructions is included in Table 1. The plasmids were transformed in MTB by conjugation using a helper strain, *E. coli* WM3064 (19).

Biodetection experiments. Bacterial cells were grown in their respective media with kanamycin until reaching the stationary phase. The bacterial cultures were dispatched in 96-well plate. Each well were supplemented with 100 µL of culture and 100 µL of growth media containing kanamycin and different metal(loid) concentrations (Ag(I), Al(III), As(III), Ba(II), Cd(II), Co(II), Cu(II), Hg(II), Mo(VI), Ni(II), Sb(III) or Zn(II)) (Table S1). The luminescence signal and OD_{600} were measured every 15 minutes over a 2 hour period with a microplate reader Infinite® 200 PRO (TECAN). The experiment was made on biological triplicates, one replicate being an independent culture. For each replicate, the luminescence signal measured without arsenite, corresponding to the background signal associated to the culture, was subtracted from the signal obtained in the presence of arsenite. The displayed results are the mean of Relative Luminescence Units normalized by OD_{600} (normalized RLU) of the triplicate and the standard deviation of the three values was calculated. The signal for one concentration is considered positive when the mean is at least twice the value of its standard deviation. Strains bearing pBBr_Lux were used as positive control to evaluate the toxicity of the sample.

Response of the bacterial biosensors after magnetic concentration. Cells from a culture of bacterial biosensor were equally distributed in 50 mL conical centrifuge tubes (10 mL by tube) before the addition of 0, 0.005, 0.01, 0.05, 0.1, 0.25, 0.5 or 1 µM of arsenite. At the bottom of the

tubes, a strong magnet (Neodymium, N48) was placed to attract bacteria. After 30 minutes, the supernatant was removed and the magnetic pellets were taken up in 200 µL of medium and deposited in a 96-well plate. The luminescence was read with a microplate reader Infinite® 200 PRO (TECAN). The experiment was repeated three times with three independent cultures each time. For each condition (magnetically concentrated or not), the luminescence signal measured without arsenite was subtracted from the signal obtained in the presence of arsenite. The results are averaged between the three replicates of the three experiments and the error is the standard error of the mean, $\sigma_m = \frac{\sigma}{\sqrt{n}}$ with σ the standard deviation and n the number of samples. A positive detection for a concentration is considered when the mean signal of the concentration is higher than twice the standard error.

Freezing-drying protocol and revival of the biosensors. To test different cryoprotectants, a culture of MSR-Pred strain (Table 1), in stationary state, was concentrated to reach OD = 20 or OD = 40 followed by an equal dilution with medium containing the cryoprotectant at a final concentration of 12.5% (w/v) sucrose, 10% (v/v) DMSO, 10 g/L mannose, 10 g/L trehalose, 10% (w/v) dehydrated milk. Solutions of cryoprotectant were previously sterilized using 0.2 µm pore size membrane filters. Cells mixed with cryoprotectant were frozen 3 hours at -80°C before freeze-drying for 24 hours. The lyophilisates were revived by addition of sterile water and incubated for 15 minutes and then diluted 5 times in growth medium with or without arsenite for luminescence measurements. The experiment was made on triplicates, one replicate being a tube of lyophilized cells. For each replicate, the luminescence signal measured without arsenite, corresponding to the background signal associated to the culture, was subtracted from the signal obtained in the presence of arsenite. The displayed results are the mean of Relative Luminescence Units normalized by OD_{600} (normalized RLU) of the triplicate and the standard deviation of the

three values was calculated. When improving freeze-drying conditions with trehalose, the same protocol was used to freeze-dry the bacteria concentrated at OD = 20 and 5% of trehalose and then revive them. The luminescence was measured on 4 lyophilized tubes in triplicate. The data was treated the same way to obtain mean of normalized RLU and standard deviation was calculated. The signal for one concentration is considered positive when the mean is at least twice the value of its standard deviation.

RESULTS AND DISCUSSION

Resistance of magnetotactic strains to arsenic. To determine the optimal microorganism to host luciferase reporters, we focused on two magnetotactic model strains: *Magnetospirillum magneticum* AMB-1 and *Magnetospirillum gryphiswaldense* MSR-1. Both environmental strains are cultivable under laboratory conditions, genetically modifiable (32, 33) and have been shown to be able to grow and absorb metal ions such as cadmium (34), cobalt, manganese and copper (35).

To facilitate simultaneous screening of many conditions, we adapted and developed the cultivation of MTB in microplates. This allowed us to grow AMB-1 and MSR-1 strains in the presence of different concentrations of arsenite and follow cell growth (OD_{600}) for 20 hours. Under these conditions, the resulting half maximal inhibitory concentrations (IC_{50}) for arsenite were determined to be 259 ± 25 µM and 406 ± 23 µM for AMB-1 and MSR-1, respectively. By comparison, the same experiment performed on cultures of an *E. coli* strain leads to an IC_{50} of 11.2 mM. These values are much higher than the WHO recommended guideline in drinking water (0.13 µM) or the French legislation for industrial effluent (0.33 µM), and are thus compatible with the use of both magnetic strains as cellular chassis for arsenic biosensors.

In some areas, arsenic concentrations can reach levels so high that they could be lethal for the biosensors. Under such conditions, their use would give a false negative result. As described for whole-cell *E. coli* biosensors (8), a control experiment is required using magnetotactic strains hosting transcriptional reporter fusions constitutively expressed (pBBr_Lux, Table 1). In the absence of luminescence signal for these control strains, the sample would simply be diluted to reach non-lethal conditions for the bacteria.

Because arsenic is likely not the only toxic compound that can be found in zones polluted by anthropogenic activity, we also estimated the resistance of both strains to a wide range of potential toxic metal(loid) ions (Cd(II), Co(II), Cu(II), Hg(II), Mo(VI), Ni(II), Sb(III)) (Table S2 in mg/L and µM). These results correspond to the first systematic quantitative measurement of MTB sensitivity to a broad range of metal(loid) ions. A comparison with *E. coli* is difficult because different methods and strains give different values in the literature (36–38), but our results clearly indicate that both MTB strains are somewhat resistant to a variety of metal(loid)s. However, since AMB-1 appears to be more sensitive than MSR-1, the latter is likely a better candidate to be used in highly polluted environments.

Search for arsenic resistance operons in AMB-1 and MSR-1. Heterologous expression in AMB-1 and MSR-1 of transcriptional reporter fusions was first investigated using the arsenic-inducible promoter P_{ars} from *E. coli*, which was previously fully characterized (8, 39). No arsenic-dependent signal was obtained from the resulting biosensors hosted in both magnetic strains (results obtained with AMB-1 are presented in Fig. S1), likely because of the phylogenic distance between *Enterobacteria* and magnetotactic *Proteobacteria*. As a consequence, an in-depth analysis of AMB-1 and MSR-1 genomes was performed, aiming at finding putative arsenic-inducible operons for the design of the magnet biosensor. We first focused on the identification of genes encoding putative ArsR regulators by a blast search against all the genome

sequence using ArsR sequence from *E. coli* as a query. As a result, ten genes in AMB-1 and eight in MSR-1 were predicted to belong to the family of ArsR-StmB regulatory proteins, a wide family of metal binding transcriptional regulators. To refine the identified targets, we analyzed whether the neighboring genes were related to known arsenic resistance operons and finally found three putative arsenic operons, one in AMB-1 genome and two in MSR-1 genome (Fig. 1).

In MSR-1, one operon (position 1,967,558 to 1,972,950 in the genome) is likely involved in the methylation of arsenic with the ArsR' repressor controlling the expression of *arsM*, a gene encoding an As(III) S-adenosylmethionine methyltransferase that could methylate arsenite up to trimethylarsenite, a volatile form of arsenic (6). Two similar operons likely involved in the export of arsenite after arsenate reduction (40, 41) were also identified in MSR-1 (from 2,246,773 to 2,251,292) and AMB-1 (from 4,062,734 to 4,063,844) genomes. In both genomes, the operons contain, in different orders, *arsR*, *arsD*, *arsA*, *arsB* and *arsC* with three copies of *arsC* in MSR-1 (*arsC1*, *arsC2* and *arsC3)*, two copies of *arsC* (*arsC1* and *arsC2)* in AMB-1 and two copies of *arsR* (*arsR1* and *arsR2)* in AMB-1. ArsR1 from AMB-1 and ArsR from MSR-1 share 75.4 % of sequence identity, and are both homologous to *E. coli* ArsR (27.1 % and 25.7 % of sequence identity, respectively). ArsR2 sequence differs more significantly (19% sequence identity with *E. coli* ArsR) but is homologous to ArsR' regulating the methylation operon in MSR-1 (80.8 % of identity), suggesting two classes of repressors in magnetospirilla that differently regulate the Ars operons. *arsC1* and *arsC2* in AMB-1 and MSR-1 both encode an arsenate reductase close to ArsC from *S. aureus* (with sequence identities between 21 to 29 %), which is predicted to use thioredoxin as an electron shuttle (42), whereas ArsC3 found in the AMB-1 operon is highly similar to *E. coli* ArsC (sequence identity of 71.1 %) which uses glutaredoxin as an electron source (43).

Transcriptional analysis of the Ars operons. The arsenic responses of the three putative operons were investigated using transcriptional approaches. AMB-1 and MSR-1 cells were first grown in the presence of 0, 50 or 200 µM arsenite, and growth curves and magnetism of the cells were monitored for 41 to 54 hours depending on the strain. No significant impact of the metalloid ion on the cell fitness and magnetic behaviors was observed between the three conditions (Fig. S2). Reverse Transcription (RT)-PCR was used to measure transcripts from the three operons between 0 and 30 hours after arsenite addition. *arsR1* and *arsC1* genes were followed for the reductase operon in both AMB-1 and MSR-1 and *arsR'* and *arsM* for the methyltransferase operon of MSR-1 (Fig. 2). *mamK* transcripts were also used as an additional control of effective magnetosome synthesis since this gene encodes an actin-like protein required for magnetosome alignment that is not known to be related to any arsenic dependency (21). Although C_{mag} measurements indicate that cell magnetism is maintained in both strains, the amount of *mamK* transcripts is not constant in AMB-1, even in absence of arsenite. These variations could be related to the unmeasured expression of Mamk-like, a homologous actin-like protein encoded in a distinct genomic islet previously identified in the genome of AMB-1 (45). As the same phenomenon is observed in all conditions and the C_{mag} is constant, we conclude arsenic is of no influence over AMB-1 magnetism.

For the AMB-1 reductase operon, induction of the transcription of *arsR1* and *arsC1* is clearly observed after 60 minutes of exposure to 50 or 200 µM arsenite (Fig. 2). As MSR-1 grow faster in our culture conditions, the first sampling was made after 40 minutes of exposure, revealing a similar result with the rapid induction of *arsR* and *arsC1*. For the two reductase operons, arsenite induction is maintained beyond 24 hours with an increase in the quantity of transcripts over time.

267 The response of the methyltransferase operon from MSR-1 is quite different. Although the
268 induction of *arsM* and *arsR*' is rapidly detected 40 minutes following the addition of metalloid
269 ions to the culture medium, no transcription is observed 2 hours or 5 hours after the addition of
270 arsenite at 50 µM or 200 µM, respectively. Both *arsRDABC* and *arsR'M* operons are thus
271 transcribed very rapidly in MSR-1, but the methylation operon is repressed in the following
272 hours, all the more rapidly as the initial metalloid concentration is low. This behavior is likely
273 related to an intracellular decrease in arsenic concentration, and would suggest that ArsR' has a
274 lower affinity for arsenic than ArsR. Despite these differences, transcriptional experiments
275 demonstrate that the promoters of the three operons identified by *in silico* analysis are all
276 regulated as a function of arsenic concentration, and as a consequence may be good candidates
277 for biosensors with a reporter gene system.

278 **Genetic construction of the biosensors.** We focused only on the reductase operon from
279 AMB-1 and the methyltransferase operon from MSR-1 in the following experiments carried out
280 to build the different biosensors. Four plasmid constructions were built by insertion of either
281 *arsR1* or *arsR'* and their respective promoters followed by two different reporter genes. The gene
282 encoding the fluorescent protein Venus was first chosen because of its small size and because it
283 was known to be functional in MTB (46–48). However, preliminary experiments performed to
284 measure the fluorescent signal in rich growth media, such as the one used for MSR-1, revealed a
285 high background noise and would require additional washing to remove growth medium in order
286 to obtain an optimal measurement. Since these additional procedures are not compatible with the
287 design of an easy-to-use biosensor, we turned to the *luxCDABE* operon as luminescent reporter
288 (8) allowing an autonomous bioluminescence emission of the luciferase enzyme without needing
289 to add any substrate in the medium. This autonomous luminescent reporter has never been used
290 in MTB, and our results demonstrate that it is fully functional in magnetospirilla (see below). The

291 corresponding plasmids harboring *luxCDABE* under the control of P*arsR1* or P*arsR'* (promoter
292 and regulator gene) were mobilized into AMB-1 and MSR-1 by conjugation, resulting in four
293 whole-cell biosensors named AMB-Pred (AMB-1 with promoter from reductase operon P*arsR1*
294 regulating *luxCDABE*), AMB-Pmet (AMB-1 with promoter from methylation operon P*arsR'*
295 regulating *luxCDABE*), MSR-Pred (MSR-1 with promoter from reductase operon P*arsR1*
296 regulating *luxCDABE*) and MSR-Pmet (MSR-1 with promoter from methylation operon P*arsR'*
297 regulating *luxCDABE*).

298 **Sensitivity and specificity of the magnetic biosensors.** Dose responses of the biosensors
299 were first characterized by monitoring the bioluminescence emission (normalized to the OD)
300 over a range of arsenite concentrations in both MTB strains harboring the two different *lux*-based
301 reporter plasmids (Fig. 3). The response time in both strains is short regardless of the promoter,
302 resulting in a significant signal measurable only 30 minutes after addition of arsenite, which
303 corresponds to one of the shortest detection times for an arsenic biosensor (7).

304 Sensitivity of the four biosensors towards arsenite differs significantly (Fig. 3A & 3B).
305 Indeed, for biosensors built with the methyltransferase-linked ArsR' promoter, a significant
306 luminescent signal is only measurable for metalloid concentrations above 5 µM in MSR-1 and
307 125 µM in AMB-1. This low sensitivity is in line with a low affinity of ArsR' for arsenic as
308 hypothesized with Reverse Transcription-PCR experiments. On the other hand, as low as 0.5 µM
309 of arsenite can be detected in both AMB-Pred and MSR-Pred, the two biosensors designed using
310 the AMB-1 identified reductase operon. These results demonstrate that the promoter selected
311 from one strain can be functional in the other one. In addition, since luminescence emission is
312 linear for both strains within a concentration range from 0.5 to 5 µM of arsenite, they can
313 therefore be used for semi-quantitative measurements of arsenite in environmental samples,
314 either by a fast detection in laboratory or in the field using a portable luminometer.

315 Metalloid specificity of the biosensors was also characterized. As arsenite (As(III)) is not
316 the only oxidation state of arsenic in water, we also tested the sensibility of the biosensors for
317 arsenate As(V). No signal was obtained for this form, either because of a low arsenate uptake in
318 MTB cells or because of a low affinity of the ArsR-repressor for arsenate as shown for example
319 in *Cupriavidus metallidurans* CH34 (49). For other metal(loid)s, the bioluminescence emission
320 was followed from AMB-Pred and MSR-Pred 30 minutes after the addition of different ions
321 species in a broad range of concentrations (0.1 to 10 µM range) (Fig. 3C & 3D). Very low to no
322 response was measured for all the common toxic metal(loid) ions tested here except for arsenite
323 and antimony. Such a dual response has already been well documented in the literature for the
324 arsenite resistance system in *E. coli* (50). As a result, the sensitivity and specificity measured for
325 AMB-Pred and MSR-Pred strains are very similar to the characteristics obtained for biosensors
326 hosted in *E. coli* (8).

327 **Biosensor performances after magnetic concentration.** Our experiments clearly indicate
328 that we developed functional unique magnetic, sensitive and specific biosensors. However, their
329 sensitivity (0,5 µM) is not low enough to detect arsenic in water intended for human consumption
330 (0,13 µM of arsenic) or even industrial effluents (0,32 µM of arsenic). To improve the detection
331 limit, we therefore exploited the magnetic character of our biosensors. The luminescence
332 emission was monitored for MSR-Pred cells incubated for 30 minutes with 5 nM to 1.0 µM of
333 arsenite in the presence of a magnet. This easy-to-do magnetic concentration step increases the
334 signal (Fig. 4), a definite advantage compared to biosensors developed in *E. coli* for which a
335 concentration step by filtration is sometimes necessary to improve the signal to noise ratio (10).
336 In addition, the magnetic concentration allows a significant improvement in the sensitivity of the
337 biosensor, allowing the detection limit to be extended from 0.5 µM to 10 nM of arsenite, which is
338 ten times lower than the drinking water standard (Fig. 4). In addition, these promising results

could be further improved by the construction of an automatic system, which would significantly reduce the experimental bias associated with manual sample handling after the magnetic concentration step.

Biosensor performances after freeze-drying. In order to use whole-cell biosensors for on-site measurements, cells have to be conditioned in latent and portable form. Freezing-drying has been successfully used to preserve functional *E. coli* whole-cell luminescent biosensors (8), but has never been described for MTB. The challenge therefore is to find the right conditions in which most bacteria remains alive. Two concentrations of MSR-Pred cells (10^{11} or 2×10^{11}) were mixed with different cryoprotectants: sucrose, dehydrated milk, DMSO, mannose or trehalose. Freeze-drying was performed for 24 hours, and cells were revived by simply adding water to the aliquots. For conditions where mannose and trehalose were used as cryoprotectants, the biosensors were capable of giving a luminescence signal after incubation with arsenite at concentration above 1 µM (Fig. 5A) whereas no signal was measured using other cryoprotectants. In both cases, cells remain magnetic after freeze-drying. For trehalose-treated cells, luminescence continued to increase over time whereas with mannose, the signal was maximized after 5 hours but subsequently decreased (Fig. S3). We therefore focused on trehalose and succeeded in improving the efficiency of freeze-drying by increasing the trehalose concentration from 10 g/L to 50 g/L and incubating the samples after revival at room temperature instead of 28 °C. A weak signal at 0.5 µM of arsenite is observed but with high variability that may be improved in the future using automatic procedures for the conservation experiments. At this stage, a detection limit of 0.75 µM of arsenite in 1.5 hours can be obtained with lyophilisates stored one week at 4 °C (Fig. 5B).

CONCLUSION

In conclusion, we have demonstrated here that magnetotactic bacteria (AMB-1 and MSR-1) are robust towards metal(loid) toxicity and can be genetically modified to produce metalloid biosensors. Arsenic was chosen as the first target analyte based on the genomic prediction of *ars* operons which transcription was subsequently shown to be induced by this toxic metalloid species. Beyond the scope of this study, this concept could be extended to other inducible metal systems known in *E. coli* such as CadR, MerR or NikR. Magnetic strains hosting *lux*-based reporter plasmids are able to give a specific bioluminescent response with a detection limit of 0.5 µM for arsenite in 30 minutes for fresh cells or 90 minutes for freeze-dried cells. In addition, the use of a cellular magnetic chassis represents a major breakthrough in the field, allowing an increase in the sensitivity threshold by a factor of 50 using a facile magnetic concentration. This improved sensitivity is lower than standards set by WHO for drinking water. Thereby, these magnetic luminescent biosensors are more efficient than *E. coli* biosensors by their increased sensitivity and their robustness regarding revitalization after freeze-drying.

These magnetic biosensors can therefore be associated with a portable luminometer to be used for *in situ* measurements. They can be hosted in semi-autonomous online water analyzers, their magnetism making it possible to avoid the problematic concentration steps on membrane, which are typically required for these analyzers to obtain a sufficient signal from non-magnetic whole-cell biosensors. The sensitivity of these magnetic biosensors can also be improved by genetic manipulation by using more intricate regulation pathways such as it has been demonstrated in *E. coli* (9, 51). In addition, as it was shown by Roda *et al*. (52), adapted microfluidic systems capable of directing, guiding or fixing the cells in specific compartments

383 can be envisaged with our system, which paves the way toward the development of ground-
384 breaking technologies in the field of whole-cell biosensors.

385 ## Supplementary data

386 Supporting information include the description of plasmids and bacterial strains used in this
387 study; solid compounds used to make metal(loid) ion solutions; primers used for plasmid
388 construction and transcriptional analysis; the response of the *E. coli* and AMB-1 biosensors built
389 using arsenic-inducible promoters from *E. coli*; AMB-1 and MSR-1 growth curves measured in
390 the presence of various concentrations of arsenite; and kinetic of the luminescent signal of MSR-
391 Pred after freeze-drying with mannose or trehalose.
392

393 ## Data availability

394 MicroScope/Genoscope. Magnetospirillum magneticum AMB-1 genome.
395 https://mage.genoscope.cns.fr/microscope/genomic/overview.php?O_id=2900 (chromosome
396 NC_007626.1)
397

398 MicroScope/Genoscope. Magnetospirillum gryphiswaldense MSR-1 v2 genome.
399 https://mage.genoscope.cns.fr/microscope/genomic/overview.php?O_id=1225 (chromosome
400 MGMSR.2)

401 Wu J., Rosen B. P., 1991. “The ArsR protein is a *trans*-acting regulatory protein”. Uniprot
402 https://www.uniprot.org/uniprot/P15905 (accession no. P15905).

Chen C.-M., Misrat T. K., Silver S., and Rosen B. P., 1986. "Nucleotide Sequence of the Structural Genes for an Anion Pump". Uniprot https://www.uniprot.org/uniprot/P08690 (accession no. P08690).

Chen C.-M., Misrat T. K., Silver S., and Rosen B. P., 1986. "Nucleotide Sequence of the Structural Genes for an Anion Pump". Uniprot https://www.uniprot.org/uniprot/P08691 (accession no. P08691).

Chen C.-M., Misrat T. K., Silver S., and Rosen B. P., 1986. "Nucleotide Sequence of the Structural Genes for an Anion Pump". Uniprot https://www.uniprot.org/uniprot/P08692 (accession no. P08692).

Wu J., Rosen B. P., 1993. "The arsD gene encodes a second trans-acting regulatory protein of the plasmid-encoded arsenical resistance operon". Uniprot https://www.uniprot.org/uniprot/P46003 (accession no. P46003).

Ji G., Silver S., 1992. "Reduction of arsenate to arsenite by the ArsC protein of the arsenic resistance operon of Staphylococcus aureus plasmid pI258." Uniprot https://www.uniprot.org/uniprot/P0A006 (accession no. P0A006).

Author information

Corresponding Author

*S.P.: Phone +33 (0)4 42 25 38 46

*D.P.: Phone +33 (0)4 42 25 30 60

Author Contributions

The manuscript was written through contributions of all authors. All authors have given approval to the final version of the manuscript.

Acknowledgements

This work was supported by a PhD grant from the CEA (Comissariat à l'Energie Atomique et aux Energies alternative). Authors would like to thank Catherine Brutesco and Géraldine Adryanczyk for technical support, Dr Hélène Javot, Dr Daniel Garcia, Dr Nicolas Ginet, Joris Tulumello and Dr Damien Faivre for fruitful scientific discussion, Dr Daniel Chevrier for proofreading of the manuscript.

References

1. Vilela CLS, Bassin JP, Peixoto RS. 2018. Water contamination by endocrine disruptors: Impacts, microbiological aspects and trends for environmental protection. Environmental Pollution 235:546–559.

2. Alimi OS, Farner Budarz J, Hernandez LM, Tufenkji N. 2018. Microplastics and Nanoplastics in Aquatic Environments: Aggregation, Deposition, and Enhanced Contaminant Transport. Environ Sci Technol 52:1704–1724.

3. Duruibe JO, Ogwuegbu MOC, Egwurugwu JN. 2007. Heavy metal pollution and human biotoxic effects. Int J Phys Sci 2:112–118.

4. Martins VV, Zanetti MOB, Pitondo-Silva A, Stehling EG. 2014. Aquatic environments polluted with antibiotics and heavy metals: a human health hazard. Environ Sci Pollut Res 21:5873–5878.

5. Melamed D. 2004. Monitoring Arsenic in the Environment: A Review of Science and Technologies for Field Measurements and Sensors 29.

6. Yan G, Chen X, Du S, Deng Z, Wang L, Chen S. 2019. Genetic mechanisms of arsenic detoxification and metabolism in bacteria. Curr Genet 65:329–338.

7. Kaur H, Kumar R, Babu JN, Mittal S. 2015. Advances in arsenic biosensor

449 development – A comprehensive review. Biosensors and Bioelectronics 63:533–545.
450 8. Prévéral S, Brutesco C, Descamps ECT, Escoffier C, Pignol D, Ginet N, Garcia D.
451 2017. A bioluminescent arsenite biosensor designed for inline water analyzer. Environ Sci Pollut
452 Res 24:25–32.
453 9. Wan X, Volpetti F, Petrova E, French C, Maerkl SJ, Wang B. 2019. Cascaded
454 amplifying circuits enable ultrasensitive cellular sensors for toxic metals. Nature Chemical
455 Biology 15:540.
456 10. Descamps ECT, Meunier D, Brutesco C, Prévéral S, Franche N, Bazin I, Miclot B,
457 Larosa P, Escoffier C, Fantino J-R, Garcia D, Ansaldi M, Rodrigue A, Pignol D, Cholat P, Ginet
458 N. 2017. Semi-autonomous inline water analyzer: design of a common light detector for
459 bacterial, phage, and immunological biosensors. Environ Sci Pollut Res Int 24:66–72.
460 11. Jouanneau S, Durand MJ, Thouand G. 2012. Online Detection of Metals in
461 Environmental Samples: Comparing Two Concepts of Bioluminescent Bacterial Biosensors.
462 Environ Sci Technol 46:11979–11987.
463 12. Balkwill DL, Maratea D, Blakemore RP. 1980. Ultrastructure of a magnetotactic
464 spirillum. Journal of Bacteriology 141:1399–1408.
465 13. Blakemore R. 1975. Magnetotactic bacteria. Science 190:377–379.
466 14. Frankel RB, Blakemore RP, Wolfe RS. 1979. Magnetite in Freshwater
467 Magnetotactic Bacteria. Science 203:1355–1356.
468 15. Smith MJ, Sheehan PE, Perry LL, O'Connor K, Csonka LN, Applegate BM,
469 Whitman LJ. 2006. Quantifying the Magnetic Advantage in Magnetotaxis. Biophys J 91:1098–
470 1107.
471 16. Dieudonné A, Pignol D, Prévéral S. 2019. Magnetosomes: biogenic iron
472 nanoparticles produced by environmental bacteria. Appl Microbiol Biotechnol 103:3637–3649.

473 17. Matsunaga T, Sakaguchi T, Tadakoro F. 1991. Magnetite formation by a magnetic
474 bacterium capable of growing aerobically. Appl Microbiol Biotechnol 35:651–655.
475 18. Schleifer KH, Schüler D, Spring S, Weizenegger M, Amann R, Ludwig W, Köhler
476 M. 1991. The Genus *Magnetospirillum* gen. nov. Description of *Magnetospirillum*
477 *gryphiswaldense* sp. nov. and Transfer of *Aquaspirillum magnetotacticum* to *Magnetospirillum*
478 *magnetotacticum* comb. nov. Systematic and Applied Microbiology 14:379–385.
479 19. Komeili A, Vali H, Beveridge TJ, Newman DK. 2004. Magnetosome vesicles are
480 present before magnetite formation, and MamA is required for their activation. PNAS 101:3839–
481 3844.
482 20. Heyen U, Schüler D. 2003. Growth and magnetosome formation by
483 microaerophilic Magnetospirillum strains in an oxygen-controlled fermentor. Appl Microbiol
484 Biotechnol 61:536–544.
485 21. Komeili A, Li Z, Newman DK, Jensen GJ. 2006. Magnetosomes are cell
486 membrane invaginations organized by the actin-like protein MamK.
487 22. Lefèvre CT, Song T, Yonnet J-P, Wu L-F. 2009. Characterization of Bacterial
488 Magnetotactic Behaviors by Using a Magnetospectrophotometry Assay. Appl Environ Microbiol
489 75:3835–3841.
490 23. Kovach ME, Elzer PH, Steven Hill D, Robertson GT, Farris MA, Roop RM,
491 Peterson KM. 1995. Four new derivatives of the broad-host-range cloning vector pBBR1MCS,
492 carrying different antibiotic-resistance cassettes. Gene 166:175–176.
493 24. Kremers G-J, Goedhart J, van Munster EB, Gadella TWJ. 2006. Cyan and Yellow
494 Super Fluorescent Proteins with Improved Brightness, Protein Folding, and FRET Förster
495 Radius,. Biochemistry 45:6570–6580.
496 25. Matsunaga T, Sakaguchi T, Tadakoro F. 1991. Magnetite formation by a magnetic

497 bacterium capable of growing aerobically. Appl Microbiol Biotechnol 35:651–655.

498 26. Komeili A, Vali H, Beveridge TJ, Newman DK. 2004. Magnetosome vesicles are
499 present before magnetite formation, and MamA is required for their activation. PNAS 101:3839–
500 3844.

501 27. Vallenet D, Calteau A, Cruveiller S, Gachet M, Lajus A, Josso A, Mercier J,
502 Renaux A, Rollin J, Rouy Z, Roche D, Scarpelli C, Médigue C. 2017. MicroScope in 2017: an
503 expanding and evolving integrated resource for community expertise of microbial genomes.
504 Nucleic Acids Res 45:D517–D528.

505 28. Waterhouse AM, Procter JB, Martin DMA, Clamp M, Barton GJ. 2009. Jalview
506 Version 2—a multiple sequence alignment editor and analysis workbench. Bioinformatics
507 25:1189–1191.

508 29. Stothard P. 2000. The Sequence Manipulation Suite: JavaScript Programs for
509 Analyzing and Formatting Protein and DNA Sequences. BioTechniques 28:1102–1104.

510 30. Petkau A, Stuart-Edwards M, Stothard P, Van Domselaar G. 2010. Interactive
511 microbial genome visualization with GView. Bioinformatics 26:3125–3126.

512 31. Chaudhary VK, Shrivastava N, Verma V, Das S, Kaur C, Grover P, Gupta A.
513 2014. Rapid Restriction Enzyme-Free Cloning of PCR Products: A High-Throughput Method
514 Applicable for Library Construction. PLoS ONE 9:e111538.

515 32. Okamura Y, Takeyama H, Sekine T, Sakaguchi T, Wahyudi AT, Sato R, Kamiya
516 S, Matsunaga T. 2003. Design and Application of a New Cryptic-Plasmid-Based Shuttle Vector
517 for Magnetospirillum magneticum. Appl Environ Microbiol 69:4274–4277.

518 33. Schultheiss D, Schüler D. 2003. Development of a genetic system for
519 Magnetospirillum gryphiswaldense. Arch Microbiol 179:89–94.

520 34. Arakaki A, Takeyama H, Tanaka T, Matsunaga T. 2002. Cadmium recovery by a

521 sulfate-reducing magnetotactic bacterium, *Desulfovibrio magneticus* RS-1, using magnetic
522 separation. Appl Biochem Biotechnol 98–100:833–840.
523 35. Tanaka M, Brown R, Hondow N, Arakaki A, Matsunaga T, Staniland S. 2012.
524 Highest levels of Cu, Mn and Co doped into nanomagnetic magnetosomes through optimized
525 biomineralisation. J Mater Chem 22:11919.
526 36. Adam V, Chudobova D, Tmejova K, Cihalova K, Krizkova S, Guran R,
527 Kominkova M, Zurek M, Kremplova M, Jimenez AMJ, Konecna M, Hynek D, Pekarik V, Kizek
528 R. 2014. An Effect of Cadmium and Lead Ions on Escherichia coli with the Cloned Gene for
529 Metallothionein (MT-3) Revealed by Electrochemistry. Electrochimica Acta 140:11–19.
530 37. Abskharon RNN, Hassan SHA, Gad El-Rab SMF, Shoreit AAM. 2008. Heavy
531 Metal Resistant of E. coli Isolated from Wastewater Sites in Assiut City, Egypt. Bull Environ
532 Contam Toxicol 81:309.
533 38. Scherer J, Nies DH. 2009. CzcP is a novel efflux system contributing to transition
534 metal resistance in Cupriavidus metallidurans CH34. Molecular Microbiology 73:601–621.
535 39. Brutesco C, Prévéral S, Escoffier C, Descamps ECT, Prudent E, Cayron J, Dumas
536 L, Ricquebourg M, Adryanczyk-Perrier G, de Groot A, Garcia D, Rodrigue A, Pignol D, Ginet
537 N. 2017. Bacterial host and reporter gene optimization for genetically encoded whole cell
538 biosensors. Environ Sci Pollut Res Int 24:52–65.
539 40. Uebe R, Schüler D. 2016. Magnetosome biogenesis in magnetotactic bacteria.
540 Nature Reviews Microbiology 14:621–637.
541 41. Mobley HLT, Rosen BP. 1982. Energetics of Plasmid-Mediated Arsenate
542 Resistance in Escherichia coli. Proceedings of the National Academy of Sciences of the United
543 States of America 79:6119–6122.
544 42. Silver S, Keach D. 1982. Energy-dependent arsenate efflux: the mechanism of

545 plasmid-mediated resistance. Proc Natl Acad Sci USA 79:6114–6118.

546 43. Ji G, Garber EAE, Armes LG, Chen C-M, Fuchs JA, Silver S. 1994. Arsenate
547 Reductase of Staphylococcus aureus Plasmid pI258. Biochemistry 33:7294–7299.

548 44. Stevens SY, Hu W, Gladysheva T, Rosen BP, Zuiderweg ERP, Lee L. 1999.
549 Secondary Structure and Fold Homology of the ArsC Protein from the Escherichia coli Arsenic
550 Resistance Plasmid R773. Biochemistry 38:10178–10186.

551 45. Rioux J-B, Philippe N, Pereira S, Pignol D, Wu L-F, Ginet N. 2010. A Second
552 Actin-Like MamK Protein in Magnetospirillum magneticum AMB-1 Encoded Outside the
553 Genomic Magnetosome Island. PLOS ONE 5:e9151.

554 46. Boucher M, Geffroy F, Prévéral S, Bellanger L, Selingue E, Adryanczyk-Perrier
555 G, Péan M, Lefèvre CT, Pignol D, Ginet N, Mériaux S. 2017. Genetically tailored magnetosomes
556 used as MRI probe for molecular imaging of brain tumor. Biomaterials 121:167–178.

557 47. Plan Sangnier A, Preveral S, Curcio A, K. A. Silva A, Lefèvre CT, Pignol D,
558 Lalatonne Y, Wilhelm C. 2018. Targeted thermal therapy with genetically engineered magnetite
559 magnetosomes@RGD: Photothermia is far more efficient than magnetic hyperthermia. Journal of
560 Controlled Release 279:271–281.

561 48. Hafsi M, Preveral S, Hoog C, Hérault J, Perrier GA, Lefèvre CT, Michel H,
562 Pignol D, Doyen J, Pourcher T, Humbert O, Thariat J, Cambien B. 2019. RGD-functionalized
563 magnetosomes are efficient tumor radioenhancers for X-rays and protons. Nanomedicine:
564 Nanotechnology, Biology and Medicine 102084.

565 49. Zhang Y-B, Monchy S, Greenberg B, Mergeay M, Gang O, Taghavi S, van der
566 Lelie D. 2009. ArsR arsenic-resistance regulatory protein from Cupriavidus metallidurans CH34.
567 Antonie van Leeuwenhoek 96:161–170.

568 50. Wang Q, Warelow TP, Kang Y-S, Romano C, Osborne TH, Lehr CR, Bothner B,

569 McDermott TR, Santini JM, Wang G. 2015. Arsenite Oxidase Also Functions as an Antimonite
570 Oxidase. Applied and Environmental Microbiology 81:1959–1965.
571 51. Jia X, Bu R, Zhao T, Wu K. 2019. Sensitive and Specific Whole-Cell Biosensor
572 for Arsenic Detection | Applied and Environmental Microbiology. Appl Environ Microbiol.
573 52. Roda A, Cevenini L, Borg S, Michelini E, Calabretta MM, Schüler D. 2013.
574 Bioengineered bioluminescent magnetotactic bacteria as a powerful tool for chip-based whole-
575 cell biosensors. Lab Chip 13:4881–4889.
576
577

578 **Fig. 1.** Representation of (A) AMB-1 and (B) MSR-1 genome maps obtained with Gview
579 (30). The location of genes involved in magnetotaxis is shown in yellow (40). The location of
580 genes encoding proteins displaying sequence similarity with *E. coli* ArsR repressor is shown in
581 brown. The location of the putative operons involved in arsenic resistance (one in AMB-1 and
582 two in MSR-1) is represented in orange with details on the putative arsenite related genes and
583 their organizations. (C) Sequence alignments obtained with Jalview (28) for the different ArsR
584 repressors identified in the potential MTB operons and the *E. coli* ArsR repressor. (D) Sequence
585 alignments obtained with Jalview for the arsenate reductase (ArsC) from MTB with ArsC from
586 *E. coli* and *S. aureus*.
587
588 **Fig. 2**. RT-PCR experiments performed in the presence of various concentrations of
589 arsenite for (A) arsR1 and arsC1 putatively involved in the reduction and export pathway
590 of arsenic in AMB-1, (B) arsR and arsC1 putatively involved in the reduction and export pathway
591 of arsenic in MSR-1 and (C) arsR' and arsM putatively involved in the methylation pathway in
592 MSR-1.
593
594 **Fig. 3.** Bioluminescence signal normalized by OD and background noise (signal without
595 arsenic) obtained after 30 minutes of exposure to different arsenite concentrations for the (A)
596 AMB-1 and (B) MSR-1 biosensors. Bioluminescence signal normalized by OD and background
597 noise (signal without metal(loid)s) obtained after 30 minutes of exposure to different metal(loid)s
598 for the (C) AMB-1 and (D) MSR-1 biosensors. The error bars are standard deviations.
599
600 **Fig. 4**. Bioluminescence signal normalized by OD and background noise (signal without
601 arsenic) for the MSR-Pred biosensor obtained after 30 minutes of incubation with arsenite in

602 presence or absence of a magnet. The results are the averages of three independent experiments
603 performed on biological triplicates each. The error bars are standard errors of the mean.
604
605 **Fig. 5.** (A) Bioluminescence signal normalized by OD and background noise (signal
606 without arsenic) obtained after 3 hours of exposure to different arsenite concentrations for the
607 freeze-dried MSR-Pred biosensor under different cryoprotecting conditions. (B) Bioluminescence
608 signal normalized by OD and background noise (signal without arsenic) obtained after 1.5 hours
609 of incubation with different arsenite concentrations for MSR-Pred freeze-dried with 50 g/L
610 trehalose and rehydrated after one week of storage at 4°C. The error bars are standard deviations.
611
612
613

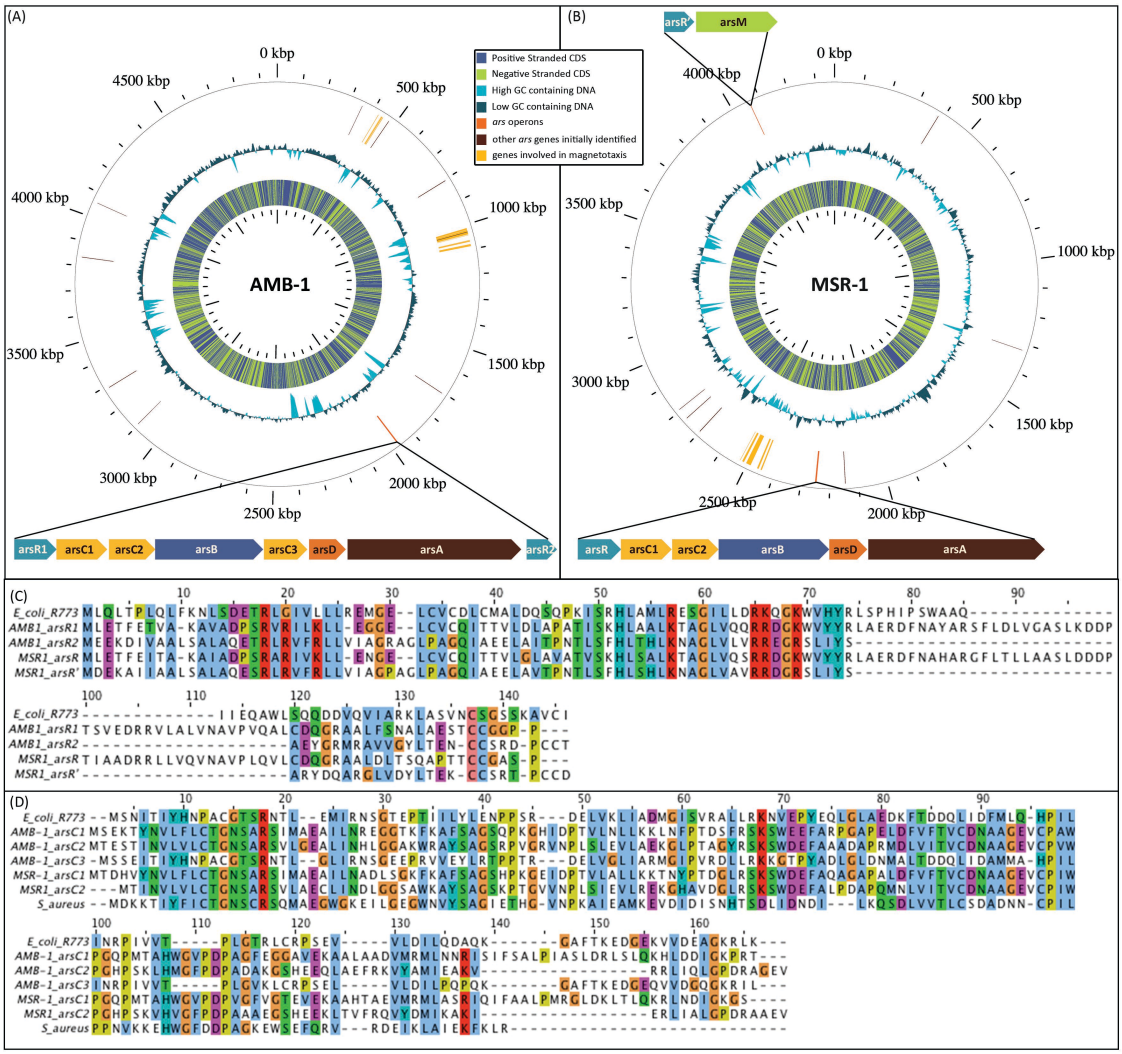

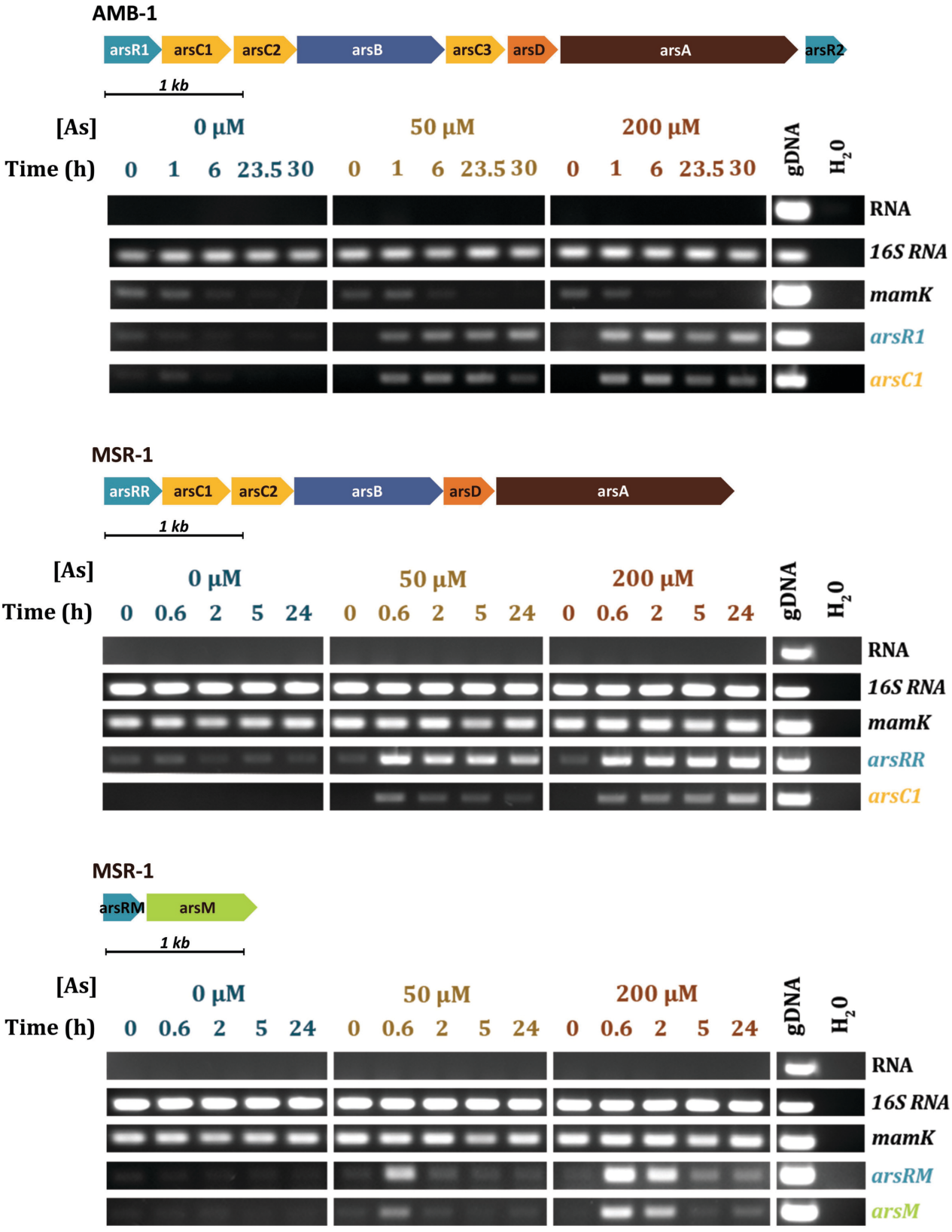

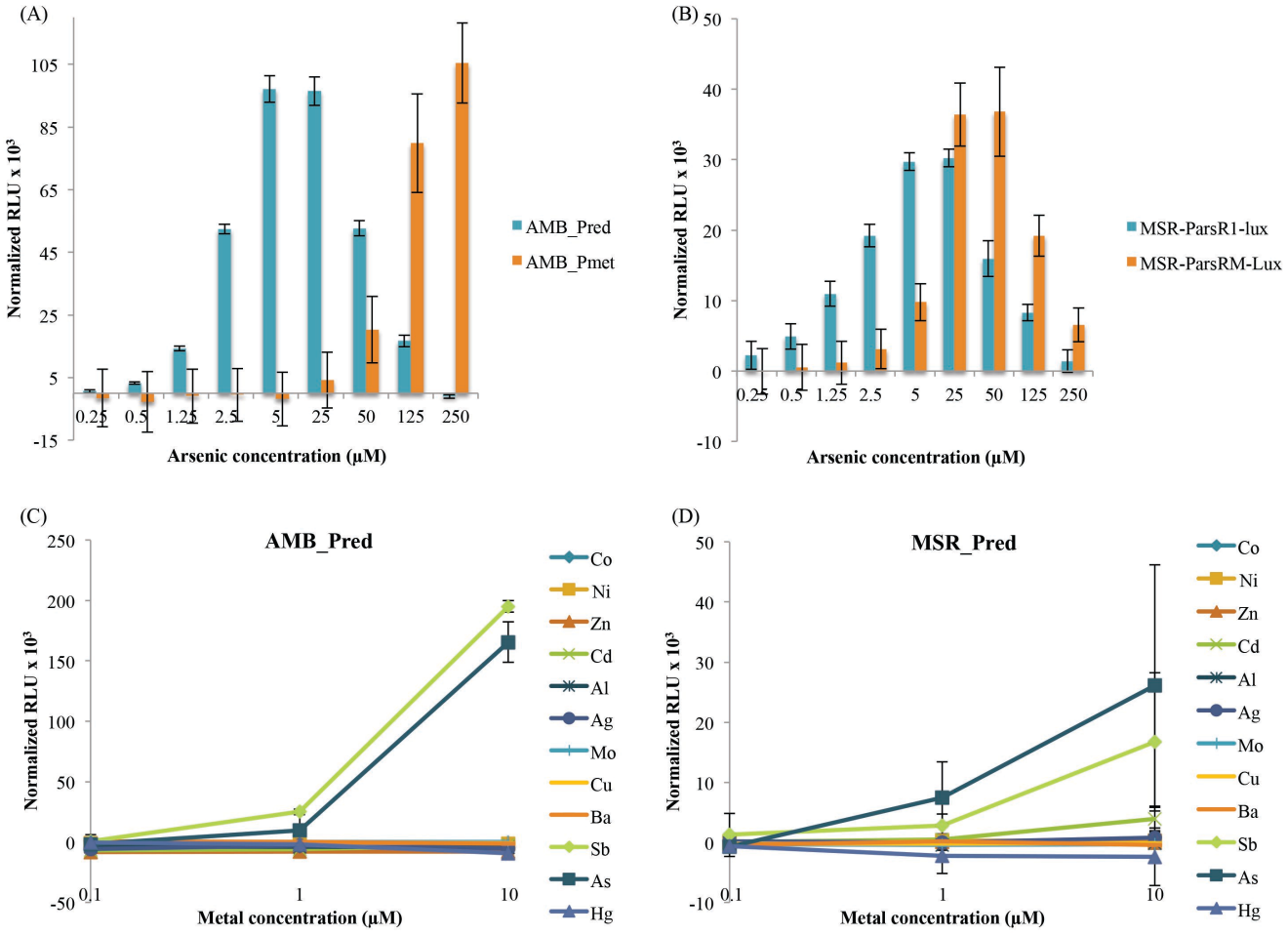

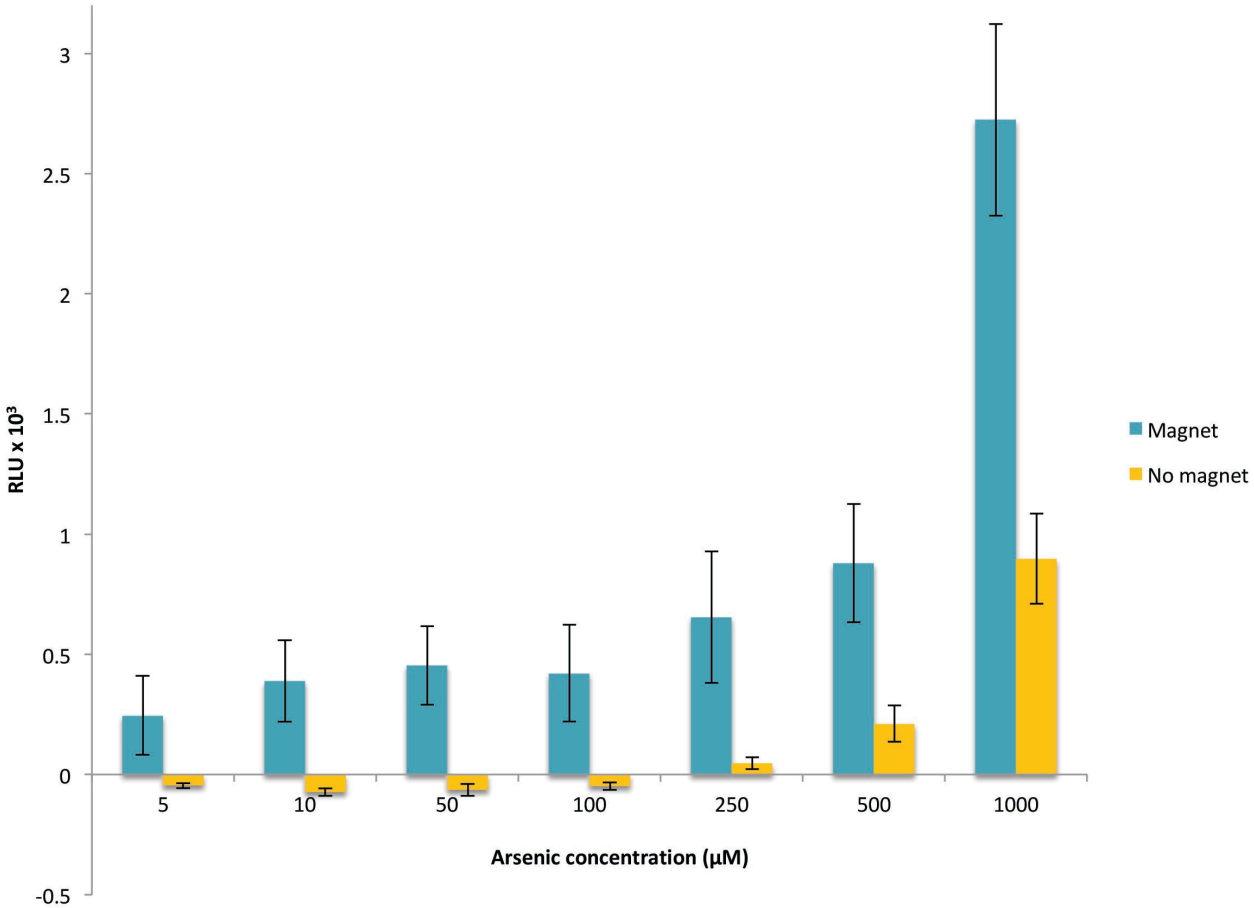

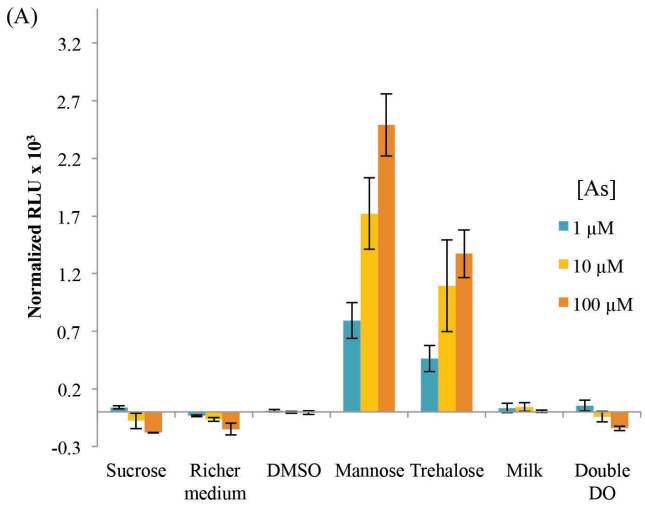

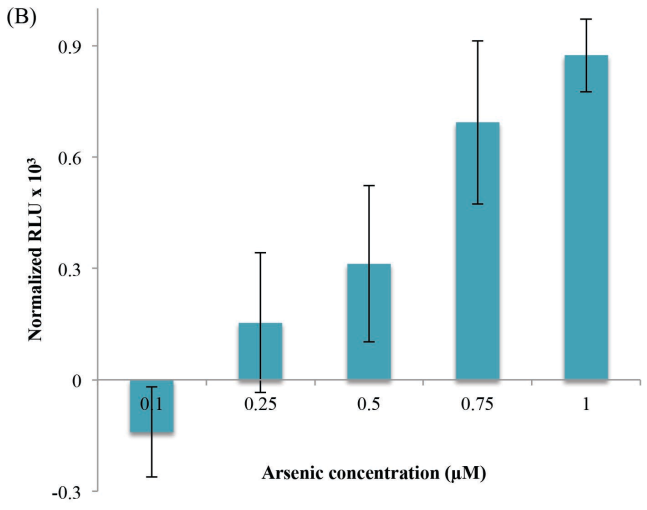

Table 1. List of (A) plasmids and (B) bacterial strain used in this study

(A)

Plasmid	Promoter	Reporter gene	Description	References
pBBR1MCS-2	T3	None	Empty plasmid, K^r	(23)
pBBr_Venus	T3	*mVenus*	Constitutive expression of mVenus fluorescence, K^r	(24)
pBBr_Lux	T3	*luxCDABE*	Constitutive expression of luminescence with the *luxCDABE* operon, K^r	This study
$pArs_{Ecoli}$_Venus	pArs + *arsR* from *E. coli*	*mVenus*	Expression of a *mVenus* gene optimized for MTB driven by an arsenic inducible promoter from *E. coli*, in K^r	(8)
$pArsR_{AMB1}$_Venus	pArs + *arsR1*	*mVenus*	Expression of a *mVenus* gene optimized for MTB driven by an arsenic inducible promoter from AMB-1, K^r	This study
$pArsR_{AMB1}$_LuxCDABE	pArs + *arsR1* AMB-1	*luxCDABE*	Expression of the *luxCDABE* operon driven by an arsenic inducible promoter from AMB-1, K^r	This study
$pArsM_{MSR1}$_Venus	pArs + *arsR'*	*mVenus*	Expression of a *mVenus* gene optimized for MTB driven by an arsenic inducible promoter from MSR-1, K^r	This study
$pArsM_{MSR1}$_LuxCDABE	pArs + *arsR'*	*luxCDABE*	Expression of the *luxCDABE* operon driven by an arsenic inducible promoter from MSR-1, K^r	This study

(B)

Strain	Plasmid	Description	References
AMB-1	None	Wild-type	(25)
MSR-1	None	Wild-type	(18)
AMB_pBBr	pBBR1-MCS2	AMB-1 negative control strain	
MSR_pBBr	pBBR1-MCS2	MSR-1 negative control strain	
AMB_Venus	pBBr_Venus	AMB-1 positive control strain	This study
MSR_Venus	pBBr_Venus	MSR-1 positive control strain	This study
AMB_Lux	pBBr_LuxCDABE	AMB-1 positive control strain	This study
MSR_Lux	pBBr_LuxCDABE	MSR-1 positive control strain	This study
AMB_pAEcoliV	$pArs_{Ecoli}$_Venus	AMB-1 fluorescent arsenic biosensor	This study
AMB_pAA1V	$pArsR1_{AMB1}$_Venus	AMB-1 fluorescent arsenic biosensor	This study
MSR_pAA1V	$pArsR1_{AMB1}$_Venus	MSR-1 fluorescent arsenic biosensor	This study
AMB_Pred	$pArsR1_{AMB1}$_LuxCDABE	AMB-1 luminescent arsenic biosensor	This study
MSR_Pred	$pArsR1_{AMB1}$_LuxCDABE	MSR-1 luminescent arsenic biosensor	This study

AMB_pAM'V	pArsM'$_{MSR1}$_Venus	AMB-1 fluorescent arsenic biosensor	This study
MSR_pAM'V	pArsM'$_{MSR1}$_Venus	MSR-1 fluorescent arsenic biosensor	This study
AMB_Pmet	pArsM'$_{MSR1}$_LuxCDABE	AMB-1 luminescent arsenic biosensor	This study
MSR_Pmet	pArsM'$_{MSR1}$_LuxCDABE	MSR-1 luminescent arsenic biosensor	This study
E_pAEcoliV	pArs$_{Ecoli}$_Venus	*E. coli* fluorescent arsenic biosensor	This study
E. coli WM3064	None	Helper strain for conjugation of MTB	(26)

Tables 2. List of primers used for amplification of (A) cDNA targets for Reverse-Transcription PCR and (B) arsenic promoters for biosensor constructions.

Name	Sequence	Target gene	Bacterium
ARN16S_AMB1_F1077	gggcactctgaagaaactgc	*16S RNA*	AMB-1
ARN16S_AMB1_R1185	gtcaccaccattgtagcacg	*16S RNA*	AMB-1
mamK_AMB1_F390	ggctcaggaggtggttcata	*mamK*	AMB-1
mamK_AMB1_R588	gagccgctcatccacatagt	*mamK*	AMB-1
arsR_AMB1_F2	tgcttgagacattcgaaaccg	*arsR1*	AMB-1
arsR_AMB1_R112	gcaccgtggtgatctggc	*arsR1*	AMB-1
arsC_AMB1_F23	cctgtttttgtgcaccggc	*arsC1*	AMB-1
arsC_AMB1_R154	gcaccgtcgggtcgatatg	*arsC1*	AMB-1
ARNr_16S_MS1_F1048	gtaccgtcatcatcgtcccc	*16S RNA*	MSR-1
ARNr16S_MSR1_R1200	cacactgggactgagacacg	*16S RNA*	MSR-1
mamK_MSR1_F773	tcgagattttgttgcggtcc	*mamK*	MSR-1
mamK_MSR1_R899	acgggcgcagtttatctttc	*mamK*	MSR-1
arsR_MSR1_2119_F272	cgacgacgatcccactatcg	*arsR1*	MSR-1
arsR_MSR1_2119_R384	ctgagacgtcaagtccaggg	*arsR1*	MSR-1
arsC_MSR1_F43	attccgcccgttcgatcatg	*arsC1*	MSR-1
arsC_MSR1_R176	ttggtcttcttcagcagggc	*arsC1*	MSR-1
arsR_MSR1_3975_F117	gaggaattggcggtcactcc	*arsR'*	MSR-1
arsR_MSR1_3975_R236	tgatcgtaacgggccgaatag	*arsR'*	MSR-1
arsM_MSR1_F595	cgacccgtaccgaattgttc	*arsM*	MSR-1
arsM_MSR1_R719	tcgcgactttctgacttggg	*arsM*	MSR-1

(B)

Name	Sequence	Target	Bacterium
pArs_AMB1_F	tatggtctctgaggtgccatgccgaccaagccgg	pArs-arsR1	AMB-1
pArs_AMB1_R	cataggtctcctcatggtggtcccccacagcag	pArs-arsR1	AMB-1
pArsM_MSR1_F	tatggtctctgagggccggtgtcgatgatgttg	pArs-arsR'	MSR-1
pArsM_MSR1_R	cataggtctcctcatggcatcctcctgttcagtcg	pArs-arsR'	MSR-1